Size distribution of SiGeC quantum dots grown on Si(311) and Si(001) surfaces

R. Jonczyk,[a] D. A. Hits, L. V. Kulik, and J. Kolodzey
Department of Electrical and Computer Engineering, University of Delaware, Newark, Delaware 19716

M. Kaba and M. A. Barteau
Department of Chemical Engineering, University of Delaware, Newark, Delaware 19716

Quantum dots of $Si_{1-x-y}Ge_xC_y$ alloys with high Ge contents were grown on Si(311) and Si(001) substrates by solid source molecular beam epitaxy and were measured by atomic force microscopy. The quantum dot layers had a nominal thickness (equivalent two-dimensional) of 4 nm. The smallest quantum dots occurred for the composition $Si_{0.09}Ge_{0.9}C_{0.01}$ on Si (311), and had a 40 nm mean diameter, an 8 nm mean height, and a density of 3.3×10^{10} cm^{-2}. Quantum dots on Si(001) were larger and had less regular spacing than quantum dots on Si(311) with the same composition. Carbon decreased both the mean size and spacing of SiGe quantum dots and the ratio of size deviation to mean diameter. The presence of small uniform quantum dots for particular compositions is attributed to a reduction in the surface migration of adatoms due to decreased atomic surface diffusivity. These results suggest that quantum dot organization is controlled by composition, substrate orientation, strain, and surface diffusion. © *1998 American Vacuum Society.* [S0734-211X(98)03803-7]

I. INTRODUCTION

Recent interest in low-dimensional nanostructures is motivated by the possibility of new electrical and optical properties compared to bulk and two-dimensional (2D) layers. Sufficiently small structures are expected to exhibit quantum confinement effects at room temperature, short propagation delays, and Terabit cm^{-2} densities.[1] Ge grows on Si by the Stranski-Krastanov mode of 2D wetting for the first 3 ML, followed by three-dimensional (3D) islanding.[2] This islanding process can be utilized to achieve self-assembled quantum dot arrays. Such self-assembled or self-organized quantum dots on Si substrates are being investigated for producing nanostructures compatible with Si circuit processing.[2] The fabrication of nanostructures by self-organization during epitaxial growth avoids the limitations of conventional lithographic processing. The question is whether the resulting quantum dot arrays will have the uniformity of sizes and positions suitable for device applications.

Quantum dot formation may be affected by substrate orientation through differences in surface energy, bond density, and diffusivity. The growth of Ge quantum dots on Si has been investigated for the Si(001),[3,4] Si(110),[5] Si(111),[6] and Si(311)[2] orientations. It has been shown that Ge layers relax more readily on Si(001) than on Si(111)[4] and maintain purely 2D growth for slightly thicker layers on Si(311) than on Si(001).[2] Additionally, the growth of SiGe quantum dots on Si(001) was found to depend on surface diffusion.[7,8] Quantum dot formation has been observed in the GeC system with optical properties depending on the C fractions.[9] The formation of Ge islands on Si can be suppressed by using surfactants such as Ga and Sb (Ref. 10) and by reducing the substrate temperature to below 300 °C.[3] Adding C to SiGe alloys adds flexibility and has been studied in thin films[11] but not previously in quantum dot layers. In this article, we report on the size distribution of SiGeC quantum dots grown on Si(311) and Si(001) surfaces, and compare the effects of composition, strain, and substrate orientation.

II. EXPERIMENT

The samples were grown by solid source molecular beam epitaxy (MBE) as described elsewhere.[11] Solid thermal sources were used for Si and Ge, and a heated graphite filament was used for C. The substrate temperature was 600 °C for all layers. X-ray diffraction indicated that these conditions typically produce single crystal epitaxial layers oriented with the substrate, for thick layers. The Si atomic fraction was varied from 0 to 0.1, and the C fraction was varied from 0 to 0.01. No surfactants, such as atomic H, were used during growth. The nominal thickness was 4 nm, which is the thickness of an equivalent flat layer having the same volume as the quantum dot layer. The compositions were inferred from growth conditions calibrated by Rutherford backscattering spectrometry and by electron microprobe measurements of thicker samples grown under identical conditions.

The layers were examined by atomic force microscopy (AFM), performed with a Digital Instruments Nanoscope III using the tapping mode technique with single crystal Si cantilevers having a nominal tip radius of 10 nm.[12] All samples were taken from the center of the wafer. To further ensure that the results were not due to local variations, several AFM scans were taken across the diameter of each wafer. The size and spacing data in Table I were obtained by analyzing the features from AFM scans. The quantum dot area was taken

[a] Electronic mail: jonczyk@ee.udel.edu

TABLE I. Nanostructure properties including composition, orientation of Si substrates, and statistical properties of quantum dots for 2 μm$\times$2 μm AFM scans of samples. Dev/dia is the standard deviation of the diameter distribution divided by the diameter.

Sample No.	Composition	Substr. orient.	Dot diameter (nm)	Peak wavl. (nm)	Dot density (cm^{-2})	Avg. dot height (nm)	Dev /dia
SGC191	$Si_{0.1}Ge_{0.9}$	(311)	70	141	7×10^9	9.1	0.86
SGC180	$Si_{0.09}Ge_{0.9}C_{0.01}$	(311)	40	64	3.4×10^{10}	7.6	0.61
SGC183	$Si_{0.1}Ge_{0.9}$	(001)	71	207	6.7×10^9	12.8	1.23
SGC181	$Si_{0.09}Ge_{0.9}C_{0.01}$	(001)	58	125	1.2×10^{10}	11.5	0.98
SGC204	Ge	(311)	105	231	2.5×10^9	16.5	0.79
SGC205	$Ge_{0.99}C_{0.01}$	(311)	95	186	3.0×10^9	15.6	0.74

at a vertical position located two times the root mean square (rms) surface roughness away from the mean base line 2D surface. The quantum dot diameter is calculated from the quantum dot area assuming a circle of the same area as the quantum dot.

III. RESULT AND DISCUSSION

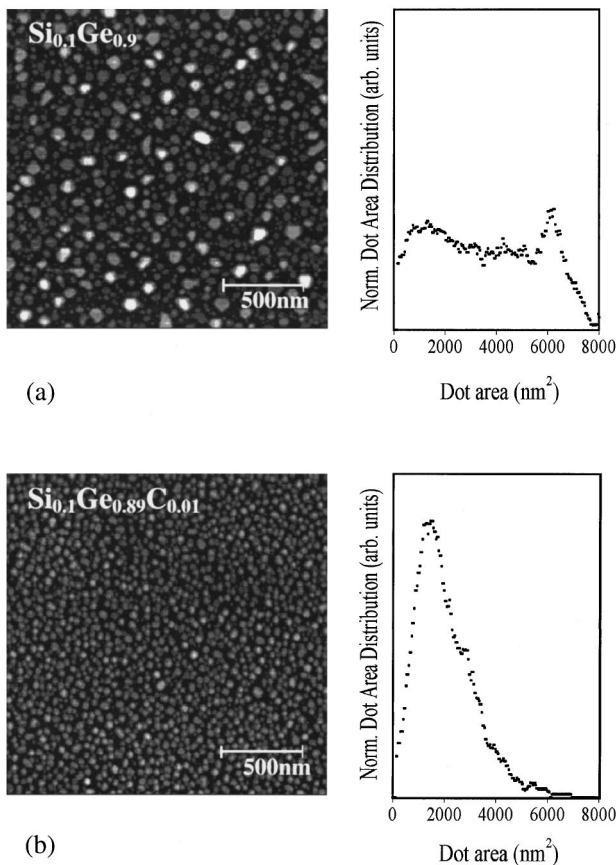Figure 1(a) shows a top view of SiGe quantum dots on Si (311) together with the quantum dot-area distribution.

(a)

(b)

FIG. 1. (a) Atomic force microscopy scan of 2 μm$\times$2 μm area of $Si_{0.1}Ge_{0.89}$ grown on (311) Si and quantum dot area distribution, (b) atomic force microscopy scan of 2 μm$\times$2 μm area of $Si_{0.1}Ge_{0.89}$ $C_{0.01}$ grown on (311) Si and quantum dot area distribution. The curves were normalized by multiplying the number of equally sized quantum dots with their area and dividing the result by the scan area.

Both large coalesced quantum dots and small coherent quantum dots are present in this sample. The size distribution shows a peak for large quantum dots at about 90 nm diameter and a somewhat broader peak for small quantum dots at 35 nm. Between these two maxima quantum dots of all sizes exist at a fairly constant rate. Quantum dots grown under similar conditions but containing C are shown in Fig. 1(b). The presence of C decreased the mean size of the quantum dots, reduced the range of feature sizes, as will be shown later by Fourier analysis, and narrowed the quantum dot size distribution to only one strong peak at 40 nm quantum dot diameter. SiGeC samples grown under identical conditions on Si(001) substrates showed that C had similar effects on the quantum dot size distribution and quantum dot feature sizes, however the effect was less pronounced than for samples grown on (311). This indicates that the substrate orientation affects the quantum dot size. The addition of C to Ge quantum dots grown on (311) substrates yielded only a slight reduction in size and quantum dot spacing. We attribute the reduced effect of C on pure Ge to low substitutional incorporation of C in Ge. Statistics for all layers discussed above are given in Table I. As indicated in Table I, over the range of compositions and substrate orientations investigated, the smallest quantum dots were obtained for SiGeC compositions on Si(311). It is also worth noting that, although smaller quantum dots are expected to have a smaller deviation of sizes, C reduced the ratio of quantum dot size deviation to quantum dot diameter, indicating higher regularity in SiGe layers containing C.

To determine the distribution of sizes, Fourier analysis was performed. The Fourier transform is proportional to the number of occurrences of the spatial wave vector, k. The spatial wavelength, $2\pi/k$, is the characteristic length associated with periodic spatial variations, including diameters, spacings, and vertical slopes of quantum dot edges. Two types of Fourier transforms were performed on the surfaces: 2D based on the two-axis (x-y) raster scans, and one dimensional (1D) based on only the x coordinate of sequential line scans. The 2D spectrum showed circular symmetry, indicating no preferred orientation on any of the substrates. The 1D Fourier intensity power spectrum, the square of the Fourier transform, is plotted versus spatial wavelength in Fig. 2, for the quantum dots of Fig. 1. The addition of C to SiGe reduced the mean value and the relative-range deviation of the
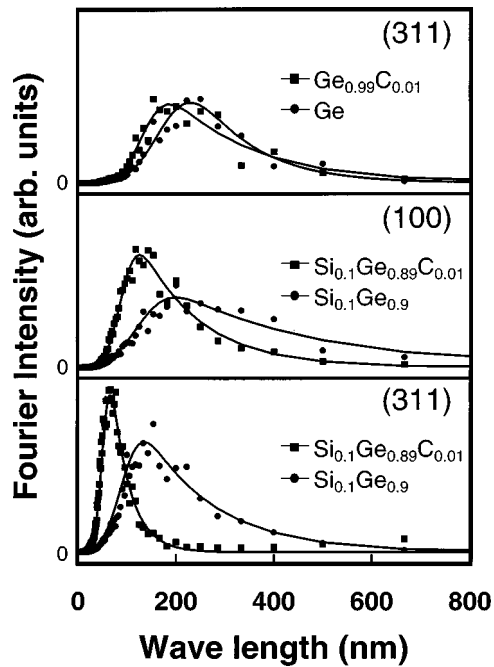
FIG. 2. Fourier intensity distribution spectrum vs quantum dot spatial wavelength for Ge, GeC, SiGe, and SiGeC quantum dots on Si(311) and Si(001), obtained from AFM scans of Fig. 1, over the 2 μm$\times$2 μm area. Markers represent measured data, solid lines were calculated by fitting the measured data to an exponentially altered Gaussian.

quantum dot wavelengths. For the same composition the Si(311) quantum dots had a smaller size and range than the Si(001) quantum dots; possible reasons for this include differences in the energies, bond densities, and atomic diffusion coefficients of the two surfaces. It is worth noting in Fig. 2 that the SiGeC (311) sample had low intensities at wavelengths from 200 to 800 nm indicating significantly more uniformity than the other samples.

It is known that the addition of Si and C to Ge reduces the lattice mismatch to the Si substrate, thus increasing the critical thickness at which Stranski-Krastanov islanding occurs. The critical thickness t_c is proportional to the misfit[13] ϵ with $t_c \propto \epsilon^{-4}$. Adding 10% Si to Ge increases the critical thickness by about 2 ML. Substitutional C will also increase the critical thickness. We believe that a higher critical thickness results in an array of quantum dots with higher quantum dot density at the thickness immediately after the transition from 2D growth to 3D growth. This and reduced surface diffusion due to the incorporation of Si and C, which reduces the average bond length of the alloy and hence increases the diffusion barrier for surface adatoms,[14] could be responsible for the more evenly distributed smaller quantum dots observed in samples containing Si and C. The increased barrier against surface diffusion will decrease the coalescence of quantum dots into larger sizes, and thus a more closely spaced distribution of smaller quantum dots will be expected. The smaller

and more regular quantum dot layers on Si(311) compared with Si(001) substrates may be due to surface-related differences including diffusivities, local strain, and critical thickness. For $Si_{0.1}Ge_{0.9}$ and $Ge_{0.99}C_{0.01}$ quantum dots under equivalent strain conditions, we found SiGe quantum dots to be smaller than GeC quantum dots, indicating that the chemical nature of the alloy affects quantum dot size in addition to strain.

IV. CONCLUSIONS

In conclusion, we have grown Ge, SiGe, GeC, and SiGeC quantum dots on (001) and (311) Si substrates. Quantum dots containing Si and C have smaller size and spacing for both (001) and (311) surfaces, and reduced deviations in size and spacing, which is crucial for applications requiring uniformity. The effect of C is stronger for alloys containing small amounts of Si, and is more prominent for alloys grown on (311) substrates. Differences between strain equivalent SiGe and GeC layers grown on (311) surfaces indicated that strain alone does not determine the geometry of quantum dot layers. These results indicate that strain, composition, and substrate orientation all play roles in quantum dot formation and provide different vehicles to control the self-assembly and self-organization of quantum dots for device applications.

[1] D. Goldhaber-Gordon, M. S. Montemerlo, J. C. Love, G. J. Opiteck, and J. C. Ellenbogen, Proc. IEEE **85**, 521 (1997).
[2] J. Knall and J. B. Pethica, Surf. Sci. **265**, 156 (1992).
[3] M. Hammar, F. K. LeGoues, J. Tersoff, M. C. Reuter, and R. M. Tromp, Surf. Sci. **349**, 129 (1996).
[4] P. W. Deelman, T. Thundat, and L. J. Schowalter, Appl. Surf. Sci. **104/105**, 510 (1996).
[5] M. Krishnamurthy, B.-K. Yang, J. D. Weil, and C. G. Slough, Appl. Phys. Lett. **70**, 49 (1997).
[6] P. D. Persans, P. W. Deelman, K. L. Stokes, L. J. Schowalter, A. Byrne, and T. Thundat, Appl. Phys. Lett. **70**, 472 (1997).
[7] P. O. Hansson, M. Albrecht, H. P. Strunk, E. Bauser, and J. H. Werner, Thin Solid Films **216**, 199 (1992).
[8] P. Schittenhelm, M. Gail, and G. Abstreiter, J. Cryst. Growth **157**, 260 (1995).
[9] M. Krishnamurthy, B.-K. Yang, and W. H. Weber, Appl. Phys. Lett. **69**, 2572 (1996).
[10] W. Kissinger, H. J. Osten, G. Lippert, B. Dietrich, and E. Bugiel, J. Appl. Phys. **76**, 8042 (1996).
[11] B. A. Orner, J. Olowolafe, K. Roe, J. Kolodzey, T. Laursen, J. W. Mayer, and J. Spear, Appl. Phys. Lett. **69**, 2557 (1996).
[12] B. A. Watson and M. A. Barteau, Chem. Mater. **6**, 771 (1994).
[13] C. W. Snyder, J. F. Mansfield, and B. G. Orr, Phys. Rev. B **46**, 9551 (1992).
[14] G. Brocks, P. J. Kelly, and R. Car, Surf. Sci. **269/270**, 860 (1991).